Revisiting time-resolved Hong-Ou-Mandel interferometry for fractional excitations

Aleksandr Latyshev[1⋆], Imen Taktak [2] and Ipsita Mandal[3] Inès Safi[1]

1 Laboratoire de Physique des Solides (UMR 5802), CNRS-Université Paris-Saclay, Bâtiment 510, 91405 Orsay, France
2 SPEC-CEA Orme des Merisiers, 91190 Gif sur Yvette
3 Department of Physics, Shiv Nadar Institution of Eminence (SNIoE), Gautam Buddha Nagar, Uttar Pradesh 201314, India

⋆ ines.safi@universite-paris-saclay.fr

Abstract

We develop a general framework for time-resolved Hong–Ou–Mandel (HOM) interferometry in the fractional quantum Hall effect (FQHE), revisiting approaches that considered only noise associated with quasiparticle tunneling. We derive a universal perturbative relation linking cross-correlations of chiral currents under arbitrary AC drives to their DC counterparts. Motivated by a recent experiments, we consider an injection protocol for pulses carrying charge q, as suggested by the plasmon-scattering approach, and show that the resulting HOM signal is entirely insensitive to any non-integer q, irrespective of the underlying edge Hamiltonian. Specializing the latter to a chiral Tomonaga–Luttinger liquid, we analyze the width of the HOM dip for both sharp and finite-duration pulses. We find that the dip width exhibits a nontrivial dependence on the scaling dimension δ, in stark contrast with the simple $1/\delta$ scaling.

Received Date
Accepted Date
Published Date

Contents

1 Introduction

Manipulating individual quasiparticles in the quantum Hall regime has opened a pathway to electronic quantum optics [1–5], where single electrons propagating along ballistic chiral edges play the role of single photons in optical media. Unlike photon optics, however, electron quantum optics is shaped by Fermi statistics and by strong Coulomb interactions, giving rise to phenomena with no optical analogue. A central tool in this field is electronic interferometry. In particular, in Hong-Ou-Mandel (HOM) geometries, synchronized sources inject excitations that collide at a quantum point contact (QPC), producing a characteristic dip in the current noise that reflects exclusion statistics [4, 6]. HOM setups have also provided clear signatures of charge fractionalization [1, 7–10] and enabled full electronic-state tomography [11–13]. HOM interferometry is now highly developed in the integer quantum Hall regime, where deterministic single-electron sources are firmly established [2–4], which is not the case in the fractional quantum Hall effect (FQHE), where it has mainly revealed quantum coherence and Fermi statistics of electron excitations [6]. In fact, time-dependent transport methods have been provided by the unifying nonequilibrium perturbative (UNEP) theory [14–21] to probe the fractional charge, traditionally extracted from DC shot noise [22–25]. By contrast, accessing fractional statistics has relied almost exclusively on DC-transport probes [26–38].

A major bottleneck is the absence of reliable on-demand anyon sources. Driven quantum dots emit only electrons, and Lorentzian voltage pulses [3] necessarily carry integer charge [39], preventing the direct generation of isolated fractional quasiparticles. This limitation has so far blocked the implementation of true single-anyon HOM interferometry in the FQHE.

Well before the development of electron quantum optics, whether through the seminal realization of on-demand single-electron emission using quantum dots in 2007 [2] or Lorentzian voltage pulses generating minimal excitations [3, 4], the possibility of shaping propagating plasmonic pulses with charge q and temporal width controlled by voltage pulses was anticipated in 1995-98 [1, 40, 41]. These works established a nonequilibrium bosonization framework in which the linear equation of motion is solved through the matrix scattering formalism for plasmons, which has since become one cornerstone of subsequent developments in quantum Hall edge states [9, 42–47].

This line of thought culminated in a recent HOM experiment [48] employing injected fractional sharp pulses, with the aim of disentangling the anyonic braiding phase θ in the time domain from its role as the scaling dimension δ. This analysis implicitly assumes a Tomonaga–Luttinger liquid (TLL) description, which however not firmly established experimentally, as already evidenced in experiments determining the fractional charge [19, 49] or fractional statistics [31–33]. In fact, the underlying TLL-based theoretical work [50] considered only the noise of the quasiparticle *tunneling* current, whereas experiments measure correlations of the *chiral* currents. All other theoretical treatments of HOM interferometry in the FQHE [51–54] share this limitation, and in several cases operate outside the domain of validity of perturbation theory (see Ref. [55]).

The distinction between chiral-current and tunneling-current correlators is crucial, and has been clarified explicitly within the formalism for nonequilibrium transport in bosonised impurity models (NETBIM), which relates the two *exactly* [19, 56–60]. This nonperturba-

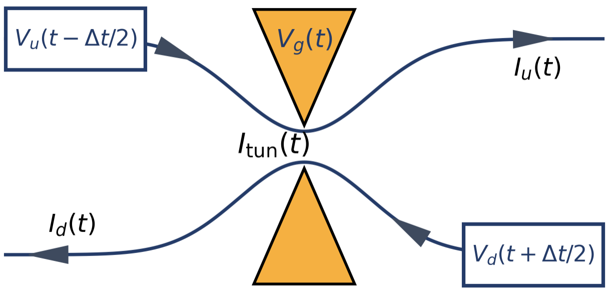

Figure 1: A QPC in the quantum Hall regime at an integer or fractional filling factor ν. We focus here on edges such that each harbors only a single chiral mode. While V_u and V_d denote the reservoir voltages, V_g denotes a gate voltage. Both the reservoir and gate voltages can be time-dependent. $I_u(t)$ and $I_d(t)$ denote the outgoing chiral current operators in the upper and lower edges [cf. Eq. (5)], respectively, and $I(t)$ represents the backscattering-current operator in Eq. (3).

tive framework transcends the TLL paradigm and accommodates arbitrary interaction ranges and profiles. Complementarily, the UNEP framework [14, 17, 20] provides a perturbative but model-agnostic route to time-dependent transport beyond bosonization, applicable to a broad class of correlated systems. UNEP relations have, in particular, enabled a unified analysis of HOM-type experiments for injected electrons across the integer and fractional quantum Hall regimes [6].

In this paper, we develop a framework for HOM interferometry in the FQHE by combining NEBIF and UNEP theory. Our contributions are threefold. First, we derive a universal perturbative relation between cross-correlations of outgoing chiral currents in the AC and DC regime, which revisits and substantially extends previous HOM analyses [51–54, 61–63]. Second, motivated by experimental evidence consistent with TLL behavior [64], we apply these relations to the TLL model and carefully analyze the short-pulse protocols used in Refs. [31, 50], showing that their interpretation requires a more refined theoretical framework. Finally, we discuss the domain of validity of our perturbative expansion [55].

Altogether, our results provide a comprehensive, drive-agnostic description of HOM interferometry in the FQHE, clarify previous theoretical inconsistencies, and yield precise predictions for the width and behavior of the HOM dip.

2 Model and perturbative relations

In this paper, we consider an icompressible chiral edge state in the FQHE at a filling factor ν in the Laughlin series. Bosonic fields $\phi_{u,d}$,are associated with the upper and lower edges of the Hall bar, respectively. The edge dynamics are governed by a quadratic bosonized Hamiltonian $\mathcal{H}_0$ in terms of $\phi_{u,d}$, without assuming the specific form of a (chiral) Tomonaga–Luttinger liquid. Quasiparticle backscattering is represented by a generic, possibly spatially extended operator A, driven by a complex time-dependent function $\tilde{p}(t,\Delta t)$. We allow here for an explicit dependence on a time shift Δt, which in the HOM setup corresponds to the relative time delay between two sources. All time-dependent forces are incorporated-either through a Keldysh gauge transformation or, equivalently, by evolving time-dependent boundary conditions [1] into $\tilde{p}(t,\Delta t)$.

Accordingly, the full time-dependent Hamiltonian takes the form

$$\mathcal{H}(t) = \mathcal{H}_0 + \mathrm{e}^{-i\omega_{\mathrm{dc}}t}\,\tilde{p}(t,\Delta t)A + \mathrm{e}^{i\omega_{\mathrm{dc}}t}\,\tilde{p}^*(t,\Delta t)A^\dagger, \tag{1}$$

Although not required in full generality, the frequency ω_{dc} often satisfies the Josephson-type relation $\omega_{\mathrm{dc}} = e^*V/\hbar$, where V denotes the applied dc voltage drop between the upper and lower edges and e^* the transferred quasiparticle charge. When considering the HOM setup, we adopt the form :

$$\tilde{p}(t,\Delta t) = e^{-i[\varphi(t-\Delta t/2)-\varphi(t+\Delta t/2)]}, \tag{2}$$

where $\varphi(t)$ describes the ac phase applied to each source, taken at the same DC voltage so that we take $\omega_{\mathrm{dc}} = 0$. We can then show that HOM noise can be expressed through noise in the DC regime, with $\varphi = 0$ and ω_{dc} finite.

Two current operators will play a central role. First, the quasiparticle tunneling current at the QPC,

$$I_{\mathrm{tun}}(t) = -i\,\frac{e^*}{\hbar}\left[\mathrm{e}^{-i\omega_{\mathrm{dc}}t}\,\tilde{p}(t,\Delta t)A - \mathrm{e}^{i\omega_{\mathrm{dc}}t}\,\tilde{p}^*(t,\Delta t)A^\dagger\right], \tag{3}$$

so that the HOM tunneling (backscattering) noise reads:

$$S^{\mathrm{HOM}}_{\mathrm{tun}}(\Delta t) = \iint_{-\infty}^{\infty} dt ds\,\langle \delta I_{\mathrm{tun}}(t)\,\delta I_{\mathrm{tun}}(t+s)\rangle\,|_{\omega_{\mathrm{dc}}=0}, \tag{4}$$

where $\delta I(t) = I(t) - \langle I(t)\rangle$. The current operator is understood to be taken in the Heisenberg representation throughout, Note that the terminology of tunneling is used purely for convenience and does not imply a bipartite structure of the system, since $\mathcal{H}_0$ is not assumed to decompose into two separate parts. In particular, interactions between the upper and lower edges are allowed.

Second, we will consider the experimentally accessible chiral edge currents,

$$I_{u,d}(x,t) = v\,\partial_x \phi_{u,d}(x,t)/\pi, \tag{5}$$

where v is the edge magnetoplasmon velocity. The corresponding cross-correlations are defined as

$$S^{\mathrm{HOM}}_{\mathrm{cr}}(\Delta t) = \iint_{-\infty}^{\infty} dt\, ds\,\langle \delta I_u(x_u,t)\,\delta I_d(x_d,t+s)\rangle\,|_{\omega_{\mathrm{dc}}=0}, \tag{6}$$

with $\delta I_\zeta(x_\zeta,t) = I_\zeta(x_\zeta,t) - \langle I_\zeta(x_\zeta,t)\rangle$ and $\zeta = u,d$. $x_{u,d}$ are the upper and lower edge measurement points The cross-correlated dc noise is defined as

$$S_{\mathrm{cr}}(\omega_{\mathrm{dc}}) = \int_{-\infty}^{\infty} ds e^{i\omega_{\mathrm{dc}}s}\,\langle \delta I_u(x_u,0)\,\delta I_d(x_d,s)\rangle\,|_{\varphi=0}, \tag{7}$$

We now focus on weak tunneling amplitudes for fractional charges. Let us recall first the UNEP relation between the HOM tunneling noise and DC noise [14, 20, 65]:

$$S^{\mathrm{HOM}}_{\mathrm{tun}}(\Delta t) = \int_{-\infty}^{+\infty} \frac{d\omega}{\Omega_0}\,|\tilde{p}(\omega,\Delta t)|^2\,S_{\mathrm{tun}}(\omega_{\mathrm{dc}} = \omega), \tag{8}$$

where $\Omega_0 = 2\pi/T_0$, with T_0 is the measurement time (larger than any relevant time scale). Interestingly, by combining UNEP theory with NEBIF, we can show a similar universal relation for cross-correlations:

$$S^{\mathrm{HOM}}_{\mathrm{cr}}(\Delta t) = \int_{-\infty}^{+\infty} \frac{d\omega}{\Omega_0}\,|\tilde{p}(\omega,\Delta t)|^2\,S_{\mathrm{cr}}(\omega_{\mathrm{dc}} = \omega), \tag{9}$$

Both relations are valid for any stationary nonequilibrium distributions, such as those induced by temperature gradients or in the "anyon collider" [66]. They also extend as well to the case $|\tilde{p}(\Delta t, t)|$ is not constrained to unity, which permits amplitude modulation, for instance from a time-dependent gate voltage (see Fig. 1).

The HOM noise is expressed as integral over the AC frequencies ω of contributions containing two factors: one associated with the drive $\tilde{p}(\omega, \Delta t)$, and the other given by $S_{\text{cr}}(\omega_{\text{dc}} = \omega)$, which retains the signature of the underlying Hamiltonian. All dependence on the time delay Δt enters exclusively through $\tilde{p}(\omega, \Delta t)$.

Let us now comment on the case one adopts an initial equilibrium thermal distribution (on which we will focus when applying Eq.(9) to a TLL model), thus $\rho_{th} \propto e^{-\beta \mathcal{H}_0}$ with electronic temperature

$$\omega_{\text{th}} = k_B T/\hbar = 1/\beta \tag{10}$$

In that case, the NETBIM, originally developed at finite frequency and DC voltages [56–59], provides exact relations between cross-correlations and backscattering noise. When combined with generalized non-equilibrium linear response theory [67], this yields an exact expression for the DC cross-correlations [60]:

$$S_{\text{cr}}(\omega_{dc}) = S_{\text{tun}}(\omega_{dc}) - 2e^* \, \omega_{th} \, G_{\text{tun}}(\omega_{dc}), \tag{11}$$

where the dc differential conductance is defined as $G_{\text{tun}}(\omega_{dc}) = \partial I_{\text{tun}}(\omega_{dc})/\partial \omega_{dc}$ with $I_{\text{tun}}(\omega_{dc})$ the DC average the tunneling current operator in Eq.(3). A similar exact form holds as well for the for the HOM noise (reported to a separate publication), leading to an exact result due to the equilibrium FDT:

$$S_{\text{cr}}^{\text{HOM}}(\Delta t = 0) = S_{\text{cr}}(\omega_{\text{dc}} = 0) = 0\,. \tag{12}$$

This vanishing, which follows directly from gauge invariance and from the perturbative expression in Eq. (9), is robust with respect to both the nature of the injected charges and the strength of interactions. It therefore cannot reveal anyonic braiding when the reservoirs act as classical sources. In setups where single electrons are injected, the disappearance of the HOM signal at $\Delta t = 0$ is interpreted as antibunching: synchronized electrons cannot collide at the QPC [6].

In the perturbative regime relevant here, the UNEP framework demonstrates the full generality of the Poissonian relation-extending well beyond bipartite systems [15, 16, 65]:

$$S_{\text{tun}}(\omega_{\text{dc}}) = e^* \coth\left(\frac{\omega_{\text{dc}}}{2\omega_{\text{th}}}\right) I_{\text{tun}}(\omega_{\text{dc}}), \tag{13}$$

where $I_{\text{tun}}(\omega_{\text{dc}})$ is the average tunneling current. As a result, $S_{\text{cr}}(\omega_{\text{dc}})$ in Eq. (11) is fixed entirely by this current, making I_{tun} the sole model-dependent ingredient entering the HOM noise in Eq. (9).

3 Application to two incident pulses

Following Refs. [40, 41] and the considerations of Ref. [61], we now consider counter-phased plasmonic pulses and derive the explicit form of the kernel $|\tilde{p}(\omega, \Delta t)|^2$ entering Eq. (9), without specifying the underlying bosonized Hamiltonian. We first address the case of extremely sharp pulses defined by:

$$\varphi(t) = 2\pi q \; \theta(t), \tag{14}$$

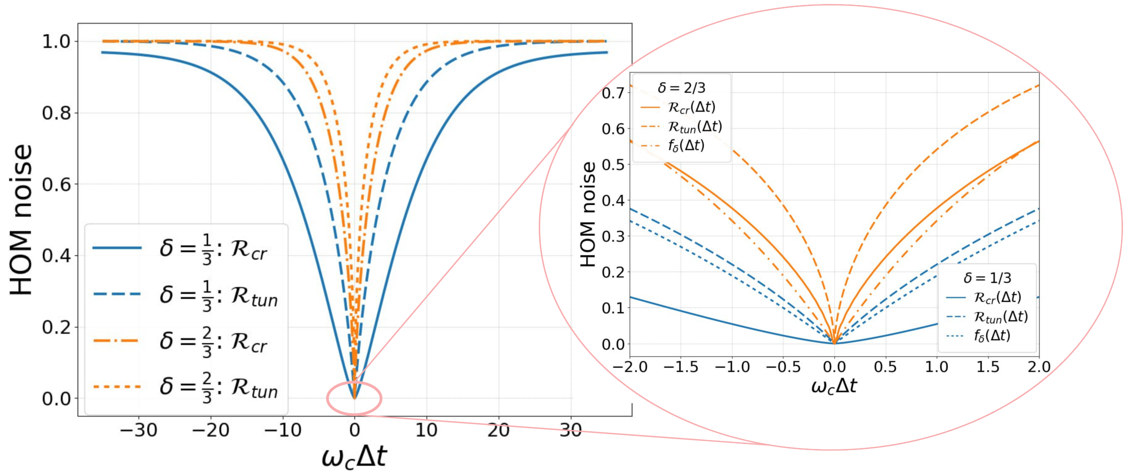

Figure 2: Normalized cross-correlated HOM noise $\mathcal{R}_{\rm cr}(\Delta t)$ and normalized tunneling noise $\mathcal{R}_{\rm tun}(\Delta t)$ from Ref. [63] as functions of $\omega_c \Delta t$ for sharp voltage pulses, for scaling dimensions $\delta = 1/3$ and $2/3$, and $\omega_{\rm th}/\omega_c = 0.1$. The results are independent of the injected non-integer dimensionless charge q. Inset: zoom of $\mathcal{R}_{\rm cr}(\Delta t)$ and $\mathcal{R}_{\rm tun}(\Delta t)$ in the vicinity of $\omega_c \Delta t = 0$. The curves are compared with the analytical short-time form $f_\delta(\Delta t) = 1 - \exp[-2\pi\omega_{\rm th}\delta|\Delta t|]$ introduced in Ref. [50].

each carrying a fractional charge q and separated by a time delay Δt. For such a drive one obtains, at nonzero frequency:

$$\tilde{p}(\omega, \Delta t) = \left(e^{2\pi i q} - 1\right) \frac{2\sin(\omega \Delta t/2)}{\omega}. \tag{15}$$

This leads to a universal oscillatory behavior of the HOM noise in Eqs.(8),(9) similarily to that in Hanbury Brown–Twiss configurations, as noted in Refs. [14, 17] for periodic pulses and in Ref. [68] for a single pulse. Let us now normalize Eq. (9) by its large-delay value $\Delta t \to \infty$, where the pulses do not overlap. We define the corresponding ratio as

$$\mathcal{R}_{\rm cr(tun)}(\Delta t) = S^{\rm HOM}_{\rm cr(tun)}(\Delta t)/S^{\rm HOM}_{\rm cr(tun)}(\Delta t \to \infty) \tag{16}$$

For sufficiently large time delays, the sources act independently and the noise reduces to the sum of two Hanbury Brown–Twiss contributions [61]. Therefore, remarkably, for noninteger q the normalized HOM signal $\mathcal{R}_{\rm cr}(\Delta t)$ is *independent of* q, since the prefactor $|e^{2\pi i q} - 1|^2$ cancels in the ratio. However, the limit $q \to$ integer is singular: in that case the HOM signal vanishes identically [68]. Remarkably, these results are robust with respect to the precise low-energy effective theory of the edges: they are controlled only by the specific sharp profile of the pulses.

It is however mor realistic to go beyond δ-like pulses and consider a finite temporal width τ, focussing here on a rectangular shape, so that the phase reads:

$$\varphi(t) = \kappa\left[t\,\theta(t) - (t-\tau)\,\theta(t-\tau)\right], \tag{17}$$

where $\kappa = 2\pi q/\tau$. A further motivation concerns the requirement of bosonization validity at low energies, below an ultraviolet cutoff ω_c. In fact extremely sharp pulses are high in energy. While Eq. (9) is general, its use within a bosonized theory requires that the integrand decays sufficiently fast above ω_c [55], a condition that depends both on the drive shape and on the intrinsic DC noise. A secure way to regularize this regime is to consider pulses of finite duration τ, much larger than the short-time cutoff $2\pi/\omega_c$. Such a single rectangular pulse can also be viewed as the limiting case of the periodic pulses employed in Ref. [48], obtained for very large period compared to τ. Fourier transforming Eq. (2), at finite frequency, yields

$$\tilde{p}(\omega,\Delta t\leq\tau)=\frac{2e^{\frac{i\omega\tau}{2}}}{\omega}\left[e^{i\kappa\Delta t}\sin\Big(\omega\frac{\tau-\Delta t}{2}\Big)-\sin\Big(\omega\frac{\tau+\Delta t}{2}\Big)\right]$$
$$+2e^{\frac{i\kappa\Delta t}{2}}\left[\frac{\sin\big((\omega+\kappa)\frac{\Delta t}{2}\big)}{\omega+\kappa}+e^{i\omega\tau}\frac{\sin\big((\omega-\kappa)\frac{\Delta t}{2}\big)}{\omega-\kappa}\right],\quad(18)$$

with the property $\tilde{p}(\omega,0)=0$. For $\Delta t>\tau$, one finds

$$\tilde{p}(\omega,\Delta t\geq\tau)=2e^{\frac{i\kappa\tau}{2}}\left[e^{\frac{i\omega}{2}(\tau-\Delta t)}\frac{\sin\big(\frac{(\omega+\kappa)\tau}{2}\big)}{\omega+\kappa}+e^{\frac{i\omega}{2}(\tau+\Delta t)}\frac{\sin\big(\frac{(\omega-\kappa)\tau}{2}\big)}{\omega-\kappa}\right]$$
$$+\frac{2e^{\frac{i\omega\tau}{2}}}{\omega}\left[\big(e^{i\kappa\tau}-1\big)\sin\Big(\frac{\omega}{2}(\Delta t-\tau)\Big)-2\cos\Big(\frac{\omega\Delta t}{2}\Big)\sin\Big(\frac{\omega\tau}{2}\Big)\right].\quad(19)$$

For a meaningful interpretation in terms of single injected excitations, the regime $\Delta t>\tau$ is the more relevant, as it avoids overlap between two incident pulses. In the narrow-pulse limit $\tau\to 0$, this expression reduces to Eq. (15). In contrast to that equation, for finite τ the limit $q\to$ integer yields a finite kernel, allowing a controlled comparison between integer and fractional q. We see clearly that the kernel depends on the width τ, whether q is fractional or integer, leading to a dependence of $\mathcal{R}_{\text{cr}}(\Delta t)$ on τ. Now we make this dependence more explicit within the TLL model.

4 Case of a TLL model

The vast majority of theoretical studies of Hall edge states rely on low-energy effective theories below the UV cutoff ω_c. When tunneling of a single quasiparticle species dominates, it is governed by one scaling dimension δ, which plays the role of the TLL parameter, and is affected by nonuniversal features such as inter-edge interactions or edge reconstruction. For definiteness, we assume quasiparticle tunneling localized at $x=0$. We also specify to a thermal initial state $\rho_{th}\propto e^{-\beta\mathcal{H}_0}$ with electronic temperature in Eq.(10). One expects a quantum metal–insulator transition at an energy scale that separates the weak- and strong-backscattering regimes [69,70], and the exact realtion in Eq.(11) is valid for all energy scales, thus in both regimes. Here we focus on the metallic one, where DC voltage or temperature scales are high enough compared to the crossover energy scale. In this case, the DC current is given by [71] :

$$I_{\text{tun}}(\omega_{\text{dc}})=\frac{2\omega_{\text{th}}}{\Gamma^2(\delta)}G_{\text{tun}}(0)\sinh(\pi\mu)\,|\Gamma(\delta+i\mu)|^2\ \text{with}\quad\mu=\frac{\omega_{\text{dc}}}{2\pi\omega_{\text{th}}}.\quad(20)$$

Here

$$G_{\text{tun}}(0)=\frac{e^*R}{2\pi}\frac{\Gamma^2(\delta)}{\Gamma(2\delta)}(2\pi)^{4(\delta-1)}\left(\frac{\omega_{\text{th}}}{\omega_c}\right)^{2(\delta-1)},\quad(21)$$

is the equilibrium conductance, with $R\ll 1$, so that e^*R is its value for $\delta=1$. Using Eq.(13) and (11) gives the DC cross-correlations:

This yields [72]

$$S_{\text{cr}}(\omega_{\text{dc}})=\frac{e^*}{\pi}I_{\text{tun}}(\omega_{\text{dc}})\Im\psi(\delta+i\mu)\quad(22)$$

where Im[...] denotes the imaginary part, and ψ is the digamma function.

For $\delta > 1/2$ $S_{\rm cr}(\omega)$ decays too slowly at $T=0$, $S_{\rm cr}(\omega) \propto |\omega/\omega_c|^{2\delta-1}$. Thus, in order to use this TLL expression, the kernel $|\tilde{p}(\omega,\Delta t|^2$ in Eq. (9) must decay rapidly, requiring $\omega_c \Delta t \gg 2\pi$. Using Eq. (9), we now analyze the HOM noise under sharp pulses. This case is directly motivated by the recent experiment in Ref. [48] where charges $Ne/3$ (i.e., $q = N/3$) were injected at $\nu = 1/3$ in order to determine the anyonic braiding phase θ.

4.1 Analysis of the HOM dip width for sharp pulses

For $N = 1$ ($q = 1/3$), the HOM dip width was claimed to scale as $1/\omega_{th}\delta$, thereby providing a direct probe of δ. For $N = 3$, one inject purely electronic pulses that do not braid whose width is claimed to determine the HOM dip width. The contrast between the $N = 1$ and $N = 3$ cases was then interpreted as a manifestation of anyonic braiding of the injected excitations with thermally created quasiparticle–quasihole pairs at the QPC, from which $\theta = 2\pi/3$ was inferred. This analysis is based on Ref. [61] claiming that while integer-charge pulses yield a dip controlled by their width, sharp fractional-charge pulses lead to a backscattering normalized noise $\mathcal{R}_{\rm tun}(\Delta t)$ approximated by

$$f_\delta(\Delta t) = 1 - \exp(-2\pi\omega_{\rm th}\delta|\Delta t|) \tag{23}$$

We start by discussing the validity of this approximation for the tunneling HOM noise, then give both analytic and numerical analysis of the HOM dip width for the more relevant chiral cross correlations.

4.1.1 HOM dip for tunneling noise

The analytical expression for the normalized $\mathcal{R}_{\rm tun}(\Delta t)$ was obtained in Ref. [63]

$$\mathcal{R}_{\rm tun}(\Delta t) = \frac{\mathcal{N}(\Delta t,\delta)}{\mathcal{D}(\delta)} = \frac{\int_0^{|\Delta t|} dt B_{e^{-2\pi\omega_{\rm th}t}}(\delta, 1-2\delta)}{\int_0^{\infty} dt B_{e^{-2\pi\omega_{\rm th}t}}(\delta, 1-2\delta)}, \tag{24}$$

where $B_z(a,b)$-is the incomplete beta function. As evident from Fig. 2, the normalized tunneling noise exhibits substantial deviations from the function $f_{\delta=2/3}(\Delta t)$ in Eq.(23). Interestingly, for $\delta = 2/3$ the corresponding cross-correlated normalized HOM noise $\mathcal{R}_{\rm cr}(\Delta t)$ follows $f_\delta(\Delta t)$ much more closely, as shown in Fig. 2, which may account for the experimentally observed behavior of $\mathcal{R}_{\rm cr}(\Delta t)$. In contrast, for the smaller scaling dimension $\delta = 1/3$, we find more pronounced discrepancies between $\mathcal{R}_{\rm cr}(\Delta t)$ and $\mathcal{R}_{\rm tun}(\Delta t)$. In this case, however, the tunneling contribution remains well approximated by $\mathcal{R}_{\rm tun}(\Delta t) \simeq f_{\delta=1/3}(\Delta t)$, in agreement with Ref. [50], which focuses exclusively on the tunneling noise for $\delta = 1/3$. Overall, these comparisons highlight clear and systematic deviations between the two types of normalized HOM noise.

Of course the numerical features of the HOM dip width for the tunneling noise can also be extracted from the asymptotic expression at short-time behaviour of the normalized tunneling noise defined in Eq. (24). We first consider the denominator. We introduce the dimensionless variable $y = 2\pi\omega_{\rm th}t$, then change it to the variable $u = e^{-y}$ and exchange the order of integration, so that:

$$\mathcal{D}(\delta) = \frac{1}{2\pi\omega_{\rm th}}\int_0^\infty dy\, B_{e^{-y}}(\delta, 1-2\delta) = \frac{1}{2\pi\omega_{\rm th}}\int_0^1 u^{\delta-1}(1-u)^{-2\delta}[-\log u]\, du. \tag{25}$$

Using the identity

$$\frac{\partial}{\partial a}B(a,b) = \int_0^1 u^{a-1}(1-u)^{b-1}\log u\, du, \tag{26}$$

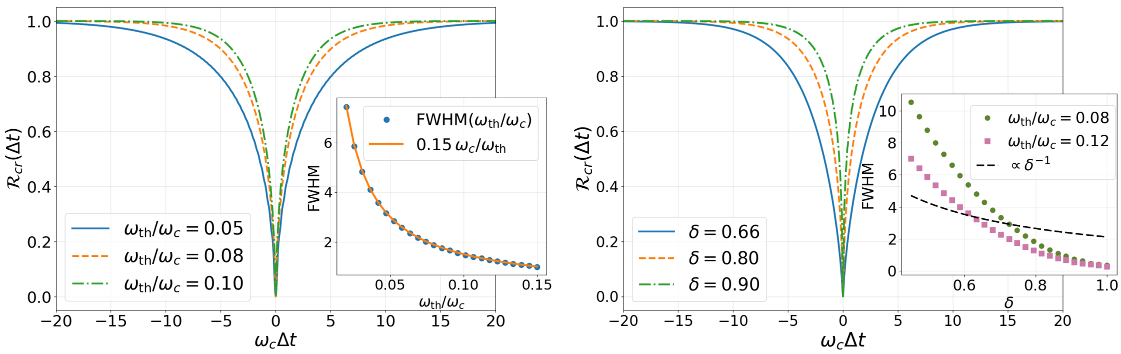

Figure 3: (Left) Normalized HOM noise $\mathcal{R}_{\rm cr}(\Delta t)$ as a function of $\omega_c \Delta t$ for sharp pulses and for different values of $\omega_{\rm th}/\omega_c = \{0.05, 0.08, 0.10\}$. Inset: numerical full width at half maximum (FWHM) of the HOM dip as a function of $\omega_{\rm th}/\omega_c$ according to a power law behavior. (Right) Normalized HOM noise $\mathcal{R}_{\rm cr}(\Delta t)$ as a function of $\omega_c \Delta t$ for sharp pulses and for different values of $\delta = \{0.66, 0.80, 0.90\}$ at $\omega_{\rm th}/\omega_c = 0.1$. Inset: numerical full width at half maximum (FWHM) of the HOM dip as a function of δ for different temperatures $\omega_{\rm th}/\omega_c = 0.08$, $\omega_{\rm th}/\omega_c = 0.12$ and comparison with the behaviour $\propto \delta^{-1}$.

we arrive at

$$\mathcal{D}(\delta) = \frac{1}{2\pi\omega_{\rm th}} B(\delta, 1-2\delta)\big[\psi(1-\delta) - \psi(\delta)\big] = \frac{1}{2\omega_{\rm th}} B(\delta, 1-2\delta)\cot(\pi\delta). \tag{27}$$

We now turn to the numerator in Eq.(24). Let us now consider $\omega_{\rm th}|\Delta t| \ll 1$. The incomplete beta function admits a regular expansion around $y = 0$ and, to leading order, we get:

$$\mathcal{N}(\Delta t, \delta) = \frac{1}{2\pi\omega_{\rm th}} \int_0^{2\pi\omega_{\rm th}|\Delta t|} B_{e^{-y}}(\delta, 1-2\delta)\, dy \simeq B(\delta, 1-2\delta)|\Delta t|. \tag{28}$$

Collecting these results, we obtain the short-time asymptotics of the normalized tunneling noise:

$$\mathcal{R}_{\rm tun}(\omega_{\rm th}|\Delta t| \to 0) = 2\,\omega_{\rm th}|\Delta t|\tan(\pi\delta), \tag{29}$$

which is obviously different from $f_\delta(\Delta t)$ in Eq.(23). Nevertheless, for small δ, the above expression reduces to

$$\mathcal{R}_{\rm tun}(\omega_{\rm th}|\Delta t|) \simeq 2\pi\omega_{\rm th}\delta|\Delta t|, \tag{30}$$

in agreement with the linear short-time behaviour of the tunneling noise in Ref. [50,63], as the function $f_\delta(\Delta t)$ can then be expanded, making such an approximation limited only to $\delta \ll 1$.

4.1.2 HOM dip width for cross-correlated noise

Now we analyse the HOM dip obtained through Eq.(9) and Eq.(22) first through a numerical analysis then from an analytic low-temperature expansion. The full width at half maximum (FWHM) of the HOM dip is shown in Fig. 3. For a fixed scaling dimension δ, the width decreases algebraically with temperature, following FWHM$(\omega_{th}) \propto 1/\omega_{th}$ in the range $\omega_{\rm th}/\omega_c = 0.07$–$0.15$, reflecting the inverse relationship between coherence time and thermal fluctuations. Consequently, even a modest rise in temperature substantially broadens the interference minimum. In contrast, for a fixed temperature $\omega_{\rm th}/\omega_c = 0.10$, it exhibits a pronounced reduction with a non-trivial dependence on δ (see inset of Fig. 3). This behaviour differs significantly from a simple $\propto \delta^{-1}$ scaling. Quantitatively, the variation with δ is significantly stronger than with ω_{th}, establishing the scaling dimension as the dominant parameter controlling the width of the HOM dip. Detailed analytical analysis of the HOM dip width for sharp pulses in Appendix A. For example it is shown that FWHM in the limit $\omega_{th}|\Delta t| \ll 1$ is given by the non-trivial function of δ:

$$\text{FWHM} \sim \frac{1}{\omega_{\text{th}}}\left[\frac{F(\infty,\delta)}{2C(\delta)}\right]^{1/(2-2\delta)}, \tag{31}$$

where

$$F(\infty,\delta) = \frac{2^{2\delta-2}}{\pi^3}\sin(\pi\delta)B(\delta,1-2\delta)[\psi'(\delta)-\psi'(1-\delta)],\ C(\delta) = \frac{\cos(\pi\delta)}{2\pi^{2\delta}(\delta-1)(2\delta-1)}, \tag{32}$$

with $\psi'(z) = d\psi(z)/dz$.

For high-order filling factors for which one has multiple edges, but where a single charge tunneling dominates with the smallest scaling parameter δ, one expects δ to reflect interedge interactions which therefore can affect the HOM dip's width [73].

4.1.3 HOM dip width for rectangular pulses

By analogy with the sharp-pulse case, we compute $\mathcal{R}_{\text{cr}}(\Delta t)$ for rectangular pulses of various durations τ, for a fractional $q = 1/3$ and integer $q = 1$ excitations as illustrated in Fig. 4. As expected, the HOM signal exhibits a strong dependence on τ, and the limit $\tau \to 0$ formally reproduces the sharp-pulse result shown in Fig. 2. This dependence holds for both fractional and integer excitations.

For integer charge $q = 1$, the HOM dip width shows only a weak sensitivity to temperature: FWHM remains nearly constant for the small values of $\tau_1 = 3.18$ Fig. 5. This insensitivity indicates that thermal broadening plays a minor role when transport is dominated by coherent single-particle processes. It is worth emphasizing that increasing the temperature leads to a progressive reduction in the discrepancy between the FWHM for fractional ($q = 1/3$) and integer ($q = 1$) excitations, as illustrated in Fig. 5. This behavior aligns with the tendency previously identified in Ref. [48].

For fractional charge $q = 1/3$, the behavior changes qualitatively. The HOM profile broadens significantly with increasing temperature, leading to a strong ω_{th}-dependence of the FWHM. This pronounced sensitivity reflects thermally assisted dephasing in the presence of fractionalized excitations. Similarly, FWHM(δ) exhibits a steep, nonlinear growth, emphasizing the key role of scaling dimension δ. The dependence on τ is also markedly stronger than for $q = 1$: at large τ, the broadening becomes superlinear, indicating that long-range correlations further smear the HOM dip.

Now we address the dependence of FWHM on the scaling dimension δ at three different values of the injected pulse duration τ. Figure 6 summarizes the results for several pulse durations τ , both for fractional ($q = 1/3$) and integer ($q = 1$) charge injection. For fractional excitations, the FWHM decreases monotonically with δ over the entire range explored. Narrow pulses ($\tau_1 = 3.183$) exhibit the steepest decay, whereas broad pulses ($\tau_2 = 9.549$) lead to a smoother, less δ-sensitive profile. This behavior reflects the dominance of high-frequency components in the correlation spectrum $S_{\text{cr}}(\omega_{\text{dc}} = \omega)$ at larger δ, which enhance temporal decoherence and compress the interference feature in time delay Δt. For integer excitations, the FWHM is nearly constant for small τ, showing only a weak residual increase with δ at larger pulse durations.

Overall, the comparison between $q = 1/3$ and $q = 1$ highlights a clear dichotomy: fractional excitations lead to pronounced scaling of the HOM dip width with δ, while integer

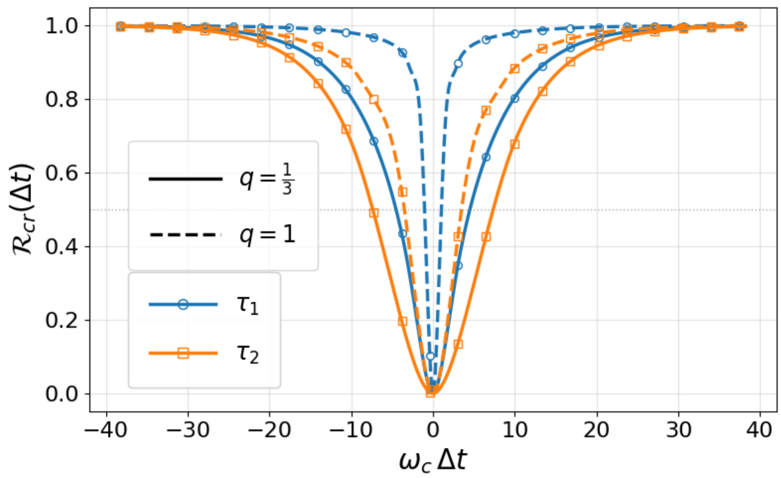

Figure 4: Normalized HOM noise $\mathcal{R}_{\text{cr}}(\Delta t)$ as a function of the delay $\omega_c\Delta t$ for rectangular pulses of finite duration $\tau_1 = 3.18$, $\tau_2 = 9.55$, for integer $q = 1$ (dashed) and fractional $q = 1/3$ (solid), respectively, at $\delta = 2/3$ and $\omega_{\text{th}}/\omega_c = 0.05$.

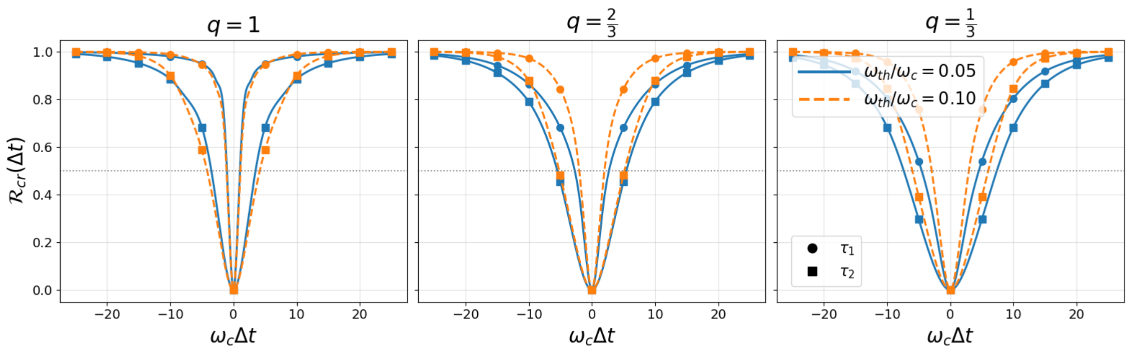

Figure 5: Normalized HOM noise $\mathcal{R}_{\text{cr}}(\Delta t)$ as a function of the delay $\omega_c\Delta t$ for rectangular pulses of finite durations $\tau_1 = 3.18$, $\tau_2 = 9.55$ for a different values of q and different temperatures $\omega_{\text{th}}/\omega_c$.

excitations yield a nearly flat baseline in the short-pulse regime. Increasing τ broadens the dip but also reduces the contrast between the two charge sectors, demonstrating how pulse shaping and quasiparticle charge jointly govern the temporal dip width of HOM interference.

5 Discussion and Conclusion

We have developed a unified theoretical framework for time-resolved Hong–Ou–Mandel (HOM) interferometry in fractional quantum Hall edge states, based on the formalism for nonequilibrium transport in bosonized impurity models (NETBIM) combined with a controlled perturbative analysis. This approach yields model-independent relations connecting photo-assisted cross-correlated noise to its dc counterpart, valid for arbitrary stationary nonequilibrium states. Two universal features emerge, independently of quasiparticle charge, statistics, or interaction strength and range: the HOM signal necessarily vanishes at zero delay, and sharp voltage pulses produce a normalized HOM response that is completely insensitive to any noninteger injected charge q. This revisits earlier interpretations based solely on tunneling-current noise and demonstrates that sharp-pulse protocols cannot provide direct access to anyonic braiding

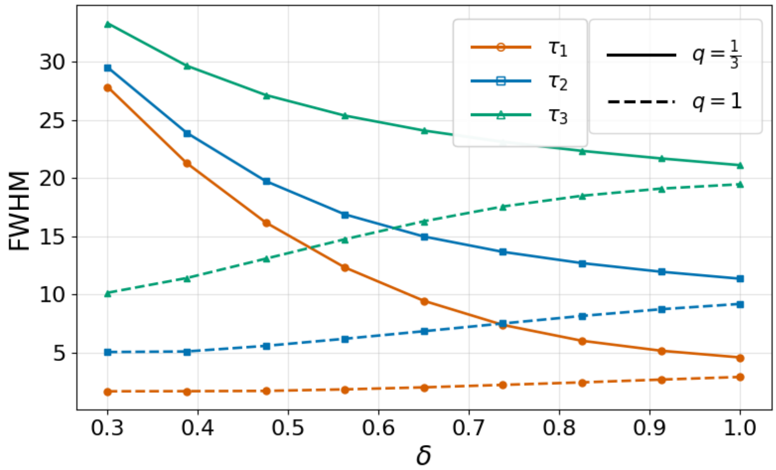

Figure 6: Full width at half maximum (FWHM) of the HOM dip versus scaling dimension δ for fractional $q = 1/3$ (solid line) and integer $q = 1$ (dashed line) at different $\tau_1 = 3.18$, $\tau_2 = 9.55$ $\tau_3 = 19.10$ and $\omega_{\text{th}}/\omega_c = 0.05$.

information.

Specializing to the chiral Tomonaga–Luttinger liquid model, we provide a detailed analysis of the HOM signal for both sharp and finite-duration rectangular pulses. We find substantial deviations from the commonly assumed $1/\delta$ scaling of the HOM dip width, whether one considers the tunneling noise, on which previous theoretical works were restricted [50–54, 63], or the experimentally relevant chiral-current noise. In Ref. [48], the value $\delta = 2/3$ was extracted using a $1/\delta$ scaling, which our results show to be accidental: this behavior is not generic and breaks down for other values of δ.

We further demonstrate that finite pulse duration introduces an additional timescale that qualitatively reshapes the HOM profile, broadens the dip, and restores sensitivity to interaction effects through the scaling dimension δ. This provides a consistent interpretation of the differences observed between integer and fractional excitations. Based on such differences, Ref. [48] inferred a time-domain braiding phase satisfying $\theta = \pi\delta$. The origin and robustness of this identity are clarified in Refs. [74, 75], which also introduce complementary strategies for determining θ.

Overall, our work provides a comprehensive and drive-agnostic framework for HOM interferometry in strongly correlated chiral systems. It clarifies the limitations of sharp-pulse injection protocols, identifies which features of the HOM dip genuinely encode interaction physics, and delivers reliable predictions for upcoming time-domain experiments targeting fractionalization and anyonic statistics in quantum Hall edge states.

As a perspective, it will be particularly interesting to apply the cross-correlation formula derived here to anyon-collider geometries or nonequilibrium anyon injection schemes that extend beyond classical AC driving. Such configurations are expected to yield a finite signal at zero time delay, potentially exposing a direct signature of anyonic statistics.

Acknowledgements

I. S. would like to acknowledge dicussions and on-going collaboration with Lucas Mazella and Seddik Ouacel.

Funding information This work was supported by the ANR grant "QuSig4QuSense" (ANR-21-CE47-0012) for I. S. and A. L.

A Asymptotic analysis of the HOM dip width for a sharp drain

In this section of the Supplemental Material, we derive a closed analytical expression for the HOM noise $S_{\text{cr}}^{\text{HOM}}(\Delta t)$,

$$S_{\text{cr}}^{\text{HOM}}(\Delta t) = \int_{-\infty}^{+\infty} \frac{d\omega}{\Omega_0} |\tilde{p}(\omega,\Delta t)|^2 S_{\text{cr}}(\omega_{\text{dc}} = \omega), \tag{A.1}$$

where $S_{\text{cr}}(\omega_{\text{dc}})$ is given by (22) and $\Omega_0 = 2\pi/T_0$. The expression for the drive kernel $|\tilde{p}(\omega,\Delta t)|^2$ is obtained from

$$|\tilde{p}(\omega,\Delta t)|^2 = \frac{1}{T_0}\int_{-T_0/2}^{T_0/2} dt \int_{-\infty}^{+\infty} ds\, e^{i\omega s} p(t+s/2)p^*(t-s/2), \tag{A.2}$$

with $p(t)$ is given by Eq. (2). For a voltage drive $V(t) = \kappa\delta(t)$, one obtain

$$|\tilde{p}(\omega,\Delta t)|^2 = 4\pi^2\delta(\omega) + \frac{1}{T_0}|e^{i\kappa}-1|^2\left(\frac{2\sin(\omega\Delta t/2)}{\omega}\right)^2, \quad \kappa = 2\pi q. \tag{A.3}$$

Substituing the expression (A.3) to (A.1) and taking into account that $S_{\text{cr}}(0) = 0$ we obtain

$$\begin{aligned} S_{\text{cr}}^{\text{HOM}}(\Delta t) = 8\sin^2(\kappa/2)\int_0^{\Delta t} d\zeta(\Delta t-\zeta)\int_{-\infty}^{+\infty}\frac{d\omega}{2\pi}\cos(\omega\zeta)S_{\text{cr}}(\omega) \\ = 8\sin^2(\kappa/2)\int_0^{\Delta t} d\zeta(\Delta t-\zeta)[\tilde{S}_{\text{cr}}(\zeta)+\tilde{S}_{\text{cr}}(-\zeta)], \end{aligned} \tag{A.4}$$

where we used the following identity

$$\frac{1-\cos(\omega\Delta t)}{\omega^2} = \int_0^{\Delta t} d\zeta(\Delta t-\zeta)\cos(\omega\zeta), \tag{A.5}$$

and $\tilde{S}_{\text{cr}}$ is the Fourier transformation of S_{cr}. In order to take this Fourier transformation we use the property of the digamma function

$$\left|\Gamma\left(\delta+\frac{i\omega}{2\pi\omega_{\text{th}}}\right)\right|^2 \Im\psi\left(\delta+\frac{i\omega}{2\pi\omega_{\text{th}}}\right) = -\pi\omega_{\text{th}}\frac{d}{d\omega}\left|\Gamma\left(\delta+\frac{i\omega}{2\pi\omega_{\text{th}}}\right)\right|^2, \tag{A.6}$$

and after integration by parts:

$$\tilde{S}_{\text{cr}}(\zeta) = \frac{e^*\omega_{\text{th}}G_{\text{tun}}(0)}{\Gamma^2(\delta)}\int_{-\infty}^{+\infty}\frac{d\omega}{2\pi}e^{-i\zeta\omega}\left\{\cosh\left(\frac{\omega}{2\omega_{\text{th}}}\right)-2i\zeta\omega_{\text{th}}\sinh\left(\frac{\omega}{2\omega_{\text{th}}}\right)\right\}\left|\Gamma\left(\delta+\frac{i\omega}{2\pi\omega_{\text{th}}}\right)\right|^2 \tag{A.7}$$

The crucial point is that the expression (A.7) contains poles solely due to the Gamma functions. By eclosing the contour and taking the corresponding poles we obtain

$$\tilde{S}_{\text{cr}}(\zeta) = \frac{e^*\omega_{\text{th}}^2 G_{\text{tun}}(0)}{\Gamma^2(\delta)}\frac{2\pi\,\Gamma(2\delta)}{2^{2\delta}\sinh^{2\delta}(\pi\omega_{\text{th}}|\zeta|)}[\cos(\pi\delta)-2|\zeta|\omega_{\text{th}}\sin(\pi\delta)]. \tag{A.8}$$

It is worth noting that the Fourier transformation (A.7) makes sense only for $\delta < 1/2$, whereas for $\delta > 1/2$ the expression should be interpreted as an analytic continuation.

Let us now analyse dependence of the HOM dip width and derive an explicit asymptotic expression for FWHM. Throughout we introduce

$$z = \omega_{\text{th}} \Delta t, \tag{A.9}$$

where ω_{th} is the thermal scale. According to (A.8) and (A.4) the normalized HOM signal is

$$\mathcal{R}_{\text{cr}}(z) = \frac{F(z;\delta)}{F(\infty;\delta)}, \qquad \mathcal{R}_{\text{cr}}(0) = 0, \qquad \mathcal{R}_{\text{cr}}(\infty) = 1, \tag{A.10}$$

where

$$F(z;\delta) = \int_0^z ds\,(z-s)K(s;\delta), \quad K(s;\delta) = \frac{\cos(\pi\delta) - 2s\sin(\pi\delta)}{\sinh^{2\delta}(\pi s)}. \tag{A.11}$$

The corresponding width is defined as FWHM$= 2\Delta t_{\text{FWHM}}$ due to symmetry, can be found as

$$\mathcal{R}(z_{\text{FWHM}}(\delta);\delta) = \frac{1}{2}, \qquad \Longleftrightarrow \qquad F(z_{\text{FWHM}}(\delta);\delta) = \frac{1}{2}F(\infty;\delta). \tag{A.12}$$

From the solution of the equation above one can obviously obtain temperature scale for the HOM dip width $\Delta t_{\text{FWHM}} \sim z_{\text{FWHM}}(\delta)/\omega_{\text{th}}$. Function $z_{\text{FWHM}}(\delta)$ has non-trivial behaviour as a function of scaling dimension δ, which also can be exctracted from the equation (A.12).

We now derive a closed analytical expression for $F(\infty,\delta)$. Starting from Eq. (A.11), one may rewrite

$$F(\infty,\delta) = \lim_{z\to\infty} \int_0^z ds\ (z-s)K(s,\delta) = -\int_0^\infty ds\ sK(s,\delta). \tag{A.13}$$

To evaluate this integral, we first note that

$$\begin{aligned}\int_0^\infty ds\ K(s,\delta) &= \left| t = e^{-2\pi s} \right| = \frac{2^{2\delta-1}}{\pi}\int_0^1 dt\ t^{\delta-1}(1-t)^{-2\delta}\left[\cos(\pi\delta) + \log t \sin(\pi\delta)/\pi\right] \\ &= \frac{2^{2\delta-1}}{\pi}B(\delta,1-2\delta)\Big\{\cos(\pi\delta) + \frac{\sin(\pi\delta)}{\pi}\underbrace{[\psi(\delta)-\psi(1-\delta)]}_{-\pi\cot(\pi\delta)}\Big\} = 0. \end{aligned} \tag{A.14}$$

Then, making the same change of variables as above one can obtain

$$\begin{aligned}F(\infty,\delta) = -\int_0^\infty ds\ sK(s,\delta) &= \frac{2^{2\delta}}{4\pi^2}\int_0^1 dt\ \left[\cos(\pi\delta) + \log t\sin(\pi\delta)/\pi\right] t^{\delta-1}(1-t)^{-2\delta}\log t \\ &= \frac{2^{2\delta-2}}{\pi^3}\sin(\pi\delta)B(\delta,1-2\delta)[\psi'(\delta)-\psi'(1-\delta)], \end{aligned} \tag{A.15}$$

where $\psi'(z) = d\psi(z)/dz$.

Then, for the $F(z,\delta)$ in the small $\omega_{\text{th}}\Delta t \to 0$ limit one can have

$$F(z,\delta) = C(\delta)\int_0^z ds\ (z-s)s^{-2\delta} = C(\delta)z^{2-2\delta}, \qquad C(\delta) = \frac{\cos(\pi\delta)}{2\pi^{2\delta}(\delta-1)(2\delta-1)}. \tag{A.16}$$

Finally, the corresponding width of the HOM dip scaled as

$$\text{FWHM} \sim \frac{1}{\omega_{\text{th}}}\left[\frac{F(\infty,\delta)}{2C(\delta)}\right]^{1/(2-2\delta)}, \tag{A.17}$$

where $C(\delta)$ and $F(\infty,\delta)$ are given by the (A.16) and (A.15).

References

[1] I. Safi, *A dynamic scattering approach for a gated interacting wire*, Eur. Phys. J. B **12**(3), 451 (1999), doi:10.1007/s100510051026.

[2] G. Fève, A. Mahé, J.-M. Berroir, T. Kontos, B. Plaçais, D. C. Glattli, A. Cavanna, B. Etienne and Y. Jin, *An on-demand coherent single-electron source*, Science **316**(5828), 1169 (2007), doi:10.1126/science.1141243.

[3] I. Klich and L. Levitov, *Quantum noise as an entanglement meter*, Phys. Rev. Lett. **102**, 100502 (2009), doi:10.1103/PhysRevLett.102.100502.

[4] J. Dubois, T. Jullien, F. Portier, P. Roche, A. Cavanna, Y. Jin, W. Wegscheider, P. Roulleau and D. C. Glattli, *Minimal-excitation states for electron quantum optics using levitons*, Nature **502**(7473), 659 (2013), doi:10.1038/nature12713.

[5] C. Grenier, R. Hervé, G. Fève and P. Degiovanni, *Electron quantum optics in quantum hall edge channels*, Modern Physics Letters B **25**(25:12n13), 1053–1073 (2011), doi:10.1142/s0217984911026772.

[6] I. Taktak, M. Kapfer, J. Nath, P. Roulleau, M. Acciai, J. Splettstoesser, I. Farrer, D. A. Ritchie and D. C. Glattli, *Two-particle time-domain interferometry in the fractional quantum Hall effect regime*, Nature Communications **13**, 5863 (2022), doi:10.1038/s41467-022-33603-3.

[7] I. P. Levkivskyi and E. V. Sukhorukov, *Dephasing in the electronic mach-zehnder interferometer at filling factor $\nu = 2$*, Phys. Rev. B **78**, 045322 (2008), doi:10.1103/PhysRevB.78.045322.

[8] V. Freulon, A. Marguerite, J. M. Berroir, B. Placais, A. Cavanna, Y. Jin and G. Fève, *Hong-ou-mandel experiment for temporal investigation of single-electron fractionalization*, Nat. Commun. **6**, 6854 EP (2015).

[9] H. Kamata, N. Kumada, M. Hashisaka, K. Muraki and T. Fujisawa, *Fractionalized wave packets from an artificial tomonaga-luttinger liquid*, Nat. Nanotechnol. **9**, 177 (2014).

[10] G. Rebora, M. Acciai, D. Ferraro and M. Sassetti, *Collisional interferometry of levitons in quantum hall edge channels at $\nu = 2$*, Phys. Rev. B **101**, 245310 (2020), doi:10.1103/PhysRevB.101.245310.

[11] C. Grenier, R. Hervé, E. Bocquillon, F. D. Parmentier, B. Plaçais, J. M. Berroir, G. Fève and P. Degiovanni, *Single-electron quantum tomography in quantum hall edge channels*, New J. Phys. **13**(9), 093007 (2011), doi:10.1088/1367-2630/13/9/093007.

[12] T. Jullien, P. Roulleau, B. Roche, A. Cavanna, Y. Jin and D. C. Glattli, *Quantum tomography of an electron*, Nature **514**, 603 (2014).

[13] R. Bisognin, A. Marguerite, B. Roussel, M. Kumar, C. Cabart, C. Chapdelaine, A. Mohammad-Djafari, J. M. Berroir, E. Bocquillon, B. Pla¸cais, A. Cavanna, U. Gennser *et al.*, *Quantum tomography of electrical currents*, Nat. Commun. **10**, 3379 (2019).

[14] I. Safi and E. V. Sukhorukov, *Determination of tunneling charge via current measurements*, Eur. Phys. Lett. **91**(6), 67008 (2010).

[15] B. Roussel, P. Degiovanni and I. Safi, *Perturbative fluctuation dissipation relation for nonequilibrium finite-frequency noise in quantum circuits*, Phys. Rev. B **93**, 045102 (2016), doi:10.1103/PhysRevB.93.045102.

[16] I. Safi, *Fluctuation-dissipation relations for strongly correlated out-of-equilibrium circuits*, Phys. Rev. B **102**, 041113 (2020), doi:10.1103/PhysRevB.102.041113.

[17] I. Safi, *Driven quantum circuits and conductors: A unifying perturbative approach*, Phys. Rev. B **99**, 045101 (2019), doi:10.1103/PhysRevB.99.045101.

[18] L.-H. Reydellet, P. Roche, D. C. Glattli, B. Etienne and Y. Jin, *Quantum partition noise of photon-created electron-hole pairs*, Phys. Rev. Lett. **90**(17), 176803 (2003), doi:10.1103/PhysRevLett.90.176803.

[19] R. Bisognin, H. Bartolomei, M. Kumar, I. Safi, J.-M. Berroir, E. Bocquillon, B. Plaçais, A. Cavanna, U. Gennser, Y. Jin and G. Fève, *Microwave photons emitted by fractionally charged quasiparticles*, Nature Communications **10**(1), 1708 (2019), doi:10.1038/s41467-019-09758-x.

[20] I. Safi, *Driven strongly correlated quantum circuits and hall edge states: Unified photoassisted noise and revisited minimal excitations*, Phys. Rev. B **106**, 205130 (2022), doi:10.1103/PhysRevB.106.205130.

[21] Feldman, D. E. and Halperin, Bertrand I., *Fractional charge and fractional statistics in the quantum hall effects*, Reports on Progress in Physics **84**(7), 076501 (2021), doi:10.1088/1361-6633/ac03aa.

[22] C. L. Kane and M. P. A. Fisher, *Nonequilibrium noise and fractional charge in the quantum hall effect*, Phys. Rev. Lett. **72**, 724 (1994).

[23] I. Safi, *Resonance in a tomonaga-luttinger liquid*, Phys. Rev. B **55**, R 12 691 (1997-II).

[24] L. Saminadayar, D. C. Glattli, Y. Jin and B. Etienne, *Direct observation of fractional charge*, Phys. Rev. Lett. **79**, 2526 (1997).

[25] R. de-Picciotto, M.Reznikov, M. Heiblum, V. Umansky, G.Bunin and D. Mahalu, *Direct observation of a fractional charge*, Nature **389**, 162 (1997).

[26] I. Safi, P. Devillard and T. Martin, *Partition Noise and statistics in the Fractional Quantum Hall Effect*, Phys. Rev. Lett. **86**, 4628 (2001).

[27] E.-A. Kim, M. Lawler, S. Vishveshwara and E. Fradkin, *Signatures of fractional statistics in noise experiments in quantum hall fluids*, Physical Review Letters **95**(17), 176402 (2005), doi:10.1103/PhysRevLett.95.176402.

[28] G. Campagnano, O. Zilberberg, I. V. Gornyi, D. E. Feldman, A. C. Potter and Y. Gefen, *Hanbury brown–twiss interference of anyons*, Phys. Rev. Lett. **109**, 106802 (2012), doi:10.1103/PhysRevLett.109.106802.

[29] C. L. Kane, *Telegraph noise and fractional statistics in the quantum hall effect*, Phys. Rev. Lett. **90**, 226802 (2003).

[30] B. Rosenow, I. P. Levkivskyi and B. I. Halperin, *Current correlations from a mesoscopic anyon collider*, Phys. Rev. Lett. **116**, 156802 (2016), doi:10.1103/PhysRevLett.116.156802.

[31] H. Bartolomei, M. Kumar, R. Bisognin, A. Marguerite, J.-M. Berroir, E. Bocquillon, B. Plaçais, A. Cavanna, Q. Dong, U. Gennser, Y. Jin and G. Fève, *Fractional statistics in anyon collisions*, Science **368**(6487), 173 (2020), doi:10.1126/science.aaz5601.

[32] P. Glidic, O. Maillet, A. Aassime, C. Piquard, A. Cavanna, U. Gennser, Y. Jin, A. Anthore and F. Pierre, *Cross-correlation investigation of anyon statistics in the $\nu = 1/3$ and $2/5$ fractional quantum hall states*, Phys. Rev. X **13**, 011030 (2023), doi:10.1103/PhysRevX.13.011030.

[33] M. Ruelle, E. Frigerio, J.-M. Berroir, B. Plaçais, J. Rech, A. Cavanna, U. Gennser, Y. Jin and G. Fève, *Comparing fractional quantum hall laughlin and jain topological orders with the anyon collider*, Phys. Rev. X **13**, 011031 (2023), doi:10.1103/PhysRevX.13.011031.

[34] H. K. Kundu, S. Biswas, N. Ofek, M. Heiblum, A. Stern and V. Umansky, *Anyonic interference and braiding phase in a mach–zehnder interferometer*, Nature Physics **19**, 515 (2023), doi:10.1038/s41567-022-01899-z.

[35] M. Thamm and B. Rosenow, *Effect of the soliton width on nonequilibrium exchange phases of anyons*, Phys. Rev. Lett. **132**, 156501 (2024), doi:10.1103/PhysRevLett.132.156501.

[36] K. Iyer, F. Ronetti, B. Grémaud, T. Martin, J. Rech and T. Jonckheere, *Finite width of anyons changes their braiding signature*, Phys. Rev. Lett. **132**, 216601 (2024), doi:10.1103/PhysRevLett.132.216601.

[37] J. Nakamura, S. Liang, G. C. Gardner and M. J. Manfra, *Impact of bulk-edge coupling on observation of anyonic braiding statistics in quantum hall interferometers*, Nature Communications **13**(1), 344 (2022).

[38] J. Nakamura, S. Liang, G. C. Gardner and M. J. Manfra, *Fabry-pérot interferometry at the $\nu = 2/5$ fractional quantum hall state*, Phys. Rev. X **13**, 041012 (2023), doi:10.1103/PhysRevX.13.041012.

[39] D. C. Glattli and P. S. Roulleau, *Levitons for electron quantum optics*, Physica Status Solidi (b) **254**(3), 1600650 (2017), doi:https://doi.org/10.1002/pssb.201600650.

[40] I. Safi and H. J. Schulz, *Transport in an inhomogeneous interacting one-dimensional system*, Phys. Rev. B **52**, R17040 (1995), doi:10.1103/PhysRevB.52.R17040.

[41] Safi, Inès, *Propriétés d'un fil quantique connecté à des fils de mesure*, Ann. Phys. Fr. **22**(5), 463 (1997), doi:10.1051/anphys:199705001.

[42] I.P. Levkivskyi and E.V. Sukhorukov, *Noise-induced phase transition in the electronic mach-zehnder interferometer*, Phys. Rev. Lett. **103**, 036801 (2009).

[43] D. B. Gutman, Y. Gefen and A. D. Mirlin, *Bosonisation out-of-equilibrium*, Europhys. Lett. **90**, 37003 (2010).

[44] B. Roussel, C. Cabart, G. Fève, E. Thibierge and P. Degiovanni, *Electron quantum optics as quantum signal processing*, Physica Status Solidi (B) **254**(3), 1600621 (2017), doi:10.1002/pssb.201600621, 1600621.

[45] E. Perfetto, G. Stefanucci, H. Kamata and T. Fujisawa, *Time-resolved charge fractionalization in inhong-ou-mandelogeneous luttinger liquids*, Phys. Rev. B **89**, 201413 (2014), doi:10.1103/PhysRevB.89.201413.

[46] H. Bartolomei, E. Frigerio, M. Ruelle *et al.*, *Time-resolved sensing of electromagnetic fields with single-electron interferometry*, Nature Nanotechnology **20**, 596 (2025), doi:10.1038/s41565-025-01888-2.

[47] H. Souquet-Basiège, B. Roussel, G. Rebora, G. Ménard, I. Safi, G. Fève and P. Degiovanni, *Quantum sensing of time-dependent electromagnetic fields with single-electron excitations*, Phys. Rev. X **15**, 031043 (2025), doi:10.1103/1nfc-stxp.

[48] M. Ruelle, E. Frigerio and *et al.*, *Time-domain braiding of anyons*, Science **389**(6755), eadm7695 (2025), doi:10.1126/science.adm7695.

[49] M. Kapfer, P. Roulleau, M. Santin, I. Farrer, D. A. Ritchie and D. C. Glattli, *A Josephson relation for fractionally charged anyons*, Science **363**(6429), 846 (2019), doi:10.1126/science.aau3539.

[50] T. Jonckheere, J. Rech, B. Grémaud and T. Martin, *Anyonic statistics revealed by the hong-ou-mandel dip for fractional excitations*, Phys. Rev. Lett. **130**, 186203 (2023), doi:10.1103/PhysRevLett.130.186203.

[51] D. Ferraro, F. Ronetti, L. Vannucci, M. Acciai, J. Rech, T. Jonckheere, T. Martin and M. Sassetti, *Hong-ou-mandel characterization of multiply charged levitons*, The European Physical Journal Special Topics **227**, 1345 (2018), doi:10.1140/epjst/e2018-800074-1.

[52] J. Rech, D. Ferraro, T. Jonckheere, L. Vannucci, M. Sassetti and T. Martin, *Minimal excitations in the fractional quantum hall regime*, Phys. Rev. Lett. **118**, 076801 (2017), doi:10.1103/PhysRevLett.118.076801.

[53] F. Ronetti, L. Vannucci, D. Ferraro, T. Jonckheere, J. Rech, T. Martin and M. Sassetti, *Crystallization of levitons in the fractional quantum hall regime*, Phys. Rev. B **98**, 075401 (2018), doi:10.1103/PhysRevB.98.075401.

[54] F. Ronetti, L. Vannucci, D. Ferraro, T. Jonckheere, J. Rech, T. Martin and M. Sassetti, *Hong-ou-mandel heat noise in the quantum hall regime*, Phys. Rev. B **99**, 205406 (2019), doi:10.1103/PhysRevB.99.205406.

[55] I. Taktak and I. Safi, *AC driven fractional quantum Hall systems: Uncovering unexpected features*, arXiv e-prints (2025), 2502.07622.

[56] C. Bena and I. Safi, *Emission and absorption noise in the fractional quantum hall effect*, Phys. Rev. B **76**, 125317 (2007), doi:10.1103/PhysRevB.76.125317.

[57] I. Safi, C. Bena and A. Crépieux, *ac conductance and nonsymmetrized noise at finite frequency in quantum wires and carbon nanotubes*, Phys. Rev. B **78**, 205422 (2008), doi:10.1103/PhysRevB.78.205422.

[58] B. Trauzettel, I. Safi, F. Dolcini and H. Grabert, *Appearance of fractional charge in the noise of nonchiral luttinger liquids*, Phys. Rev. Lett. **92**, 226405 (2004), doi:10.1103/PhysRevLett.92.226405.

[59] F. Dolcini, B. Trauzettel, I. Safi and H. Grabert, *Transport properties of single channel quantum wires with an impurity : Influence of finite length and temperature on average current and noise*, Phys. Rev. B **71**, 165309 (2005).

[60] Gu Zhang *et al*, in preparation (2025).

[61] T. Jonckheere, J. Rech, B. Grémaud and T. Martin, *Anyonic statistics revealed by the hong-ou-mandel dip for fractional excitations*, Phys. Rev. Lett. **130**, 186203 (2023), doi:10.1103/PhysRevLett.130.186203.

[62] F. Ronetti, L. Vannucci, D. Ferraro, T. Jonckheere, J. Rech, T. Martin and M. Sassetti, *Crystallization of levitons in the fractional quantum hall regime*, Phys. Rev. B **98**, 075401 (2018), doi:10.1103/PhysRevB.98.075401.

[63] S. Varada, C. Spånslätt and M. Acciai, *Exchange-phase erasure in anyonic hong-ou-mandel interferometry*, Phys. Rev. B **111**, L201407 (2025), doi:10.1103/PhysRevB.111.L201407.

[64] R. Guerrero-Suarez, A. Suresh, T. Maiti, S. Liang, J. Nakamura, G. C. Gardner, C. Chamon and M. Manfra, *Universal anyon tunneling in a chiral luttinger liquid*, ArXiv:2502.20551v2 (2025).

[65] I. Safi, *Time-dependent Transport in arbitrary extended driven tunnel junctions*, arXiv e-prints (2014), 1401.5950.

[66] Inès Safi, Imen Taktak, and Aleksander Latyshev, in preparation.

[67] I. Safi and P. Joyez, *Time-dependent theory of nonlinear response and current fluctuations*, Phys. Rev. B **84**, 205129 (2011), doi:10.1103/PhysRevB.84.205129.

[68] M. S. O. L. Mazzella and I. Safi, Unpublished (2025).

[69] C. L. Kane and M. P. A. Fisher, *Transmission through barriers and resonant tunneling in an interacting one-dimensional electron gas*, Phys. Rev. B **46**, 15233 (1992), doi:10.1103/PhysRevB.46.15233.

[70] P. Fendley, A. W. W. Ludwig and H. Saleur, *Exact conductance through point contacts in the $\nu = 1/3$ fractional quantum hall effect*, Phys. Rev. Lett. **74**, 3005 (1995), doi:10.1103/PhysRevLett.74.3005.

[71] X.-G. Wen, *Edge transport properties of the fractional quantum hall states and weak-impurity scattering of a one-dimensional charge-density wave*, Phys. Rev. B **44**, 5708 (1991), doi:10.1103/PhysRevB.44.5708.

[72] N. Schiller, T. Alkalay, C. Hong, V. Umansky, M. Heiblum, Y. Oreg and K. Snizhko, *Scaling tunnelling noise in the fractional quantum Hall effect tells about renormalization and breakdown of chiral Luttinger liquid*, arXiv e-prints (2024), 2403.17097.

[73] X.-G. Wen, *Theory of the edge states in fractional quantum Hall effects*, Int. J. Mod. Phys. B **06**(10), 1711 (1992), doi:10.1142/S0217979292000840.

[74] A. Latyshev and I. Safi, *Unexpected non-universality of the time braiding phase of anyons tied by the scaling dimension* (2025), 2510.20592.

[75] I. Safi, *Time domain braiding of anyons revealed through a nonequilibrium fluctuation dissipation theorem* (2025), 2510.10525.